ELSEVIER

Journal of Chromatography A, 773 (1997) 1–12

JOURNAL OF CHROMATOGRAPHY A

Pressure drop in centrifugal partition chromatography

Michel J. van Buel, Luuk A.M. van der Wielen*, Karel Ch.A.M. Luyben

Department of Biochemical Engineering, Delft University of Technology, Julianalaan 67, 2628 BC Delft, The Netherlands

Received 2 December 1996; revised 17 February 1997; accepted 26 March 1997

Abstract

Centrifugal partition chromatography (CPC) is more and more becoming a valuable alternative for conventional preparative chromatographic processes. Pressure drop is one of the main limitations hampering optimum performance of a CPC. A model is presented for the pressure drop over a CPC column. The pressure drop consists of two contributions: the hydrodynamic pressure drop, caused by the flow of liquid through the narrow ducts, and the hydrostatic pressure drop, caused by the difference in density between the liquids in the channels and the ducts, and by the centrifugal force. The model contains two adjustable parameters that can be obtained independently by fitting experimental pressure drop data. Two types of column geometries have been tested. The model describes the experimental data well. The total pressure drop is mainly due to the hydrostatic pressure drop.

Keywords: Centrifugal partition chromatography; Counter-current chromatography; Pressure drop

1. Introduction

Centrifugal partition chromatography (CPC) is a novel form of the well known counter-current chromatographic technique which is based on the difference in partitioning behaviour of components in a mixture over two immiscible liquid phases. In CPC one of these phases is kept stationary while the other flows through the column. To retain the stationary phase in the column, the column has a tortuous internal geometry, and is placed in a centrifugal field. As shown in Fig. 1, a CPC column consists of a series of channels engraved in a polymer plate [1]. The channels are connected by narrow ducts. Several plates are put together to form a cartridge. The cartridges are placed in the rotor of a centrifuge and are connected to form the chromatographic column. Two types of column geometries are shown in Fig. 1. The volume of the column depends on the number of cartridges placed in the rotor. A typical column consists of several hundreds to several thousands of channel–duct combinations and typical volumes range from 100 ml for laboratory scale to 30 l for production scale equipment. The mobile phase enters and leaves the column via rotary seals.

The mobile phase can either be the lighter or the denser phase. In the latter case, the mobile phase flows through the channels from the axis to the outside of the rotor, this is called the descending mode. The other case, the mobile phase flowing towards the axis, is called the ascending mode. Solutes with different partitioning behaviour, that are injected as a mixture, distribute differently over the two phases, and consequently develop different

*Corresponding author.

PII S0021-9673(97)00248-3

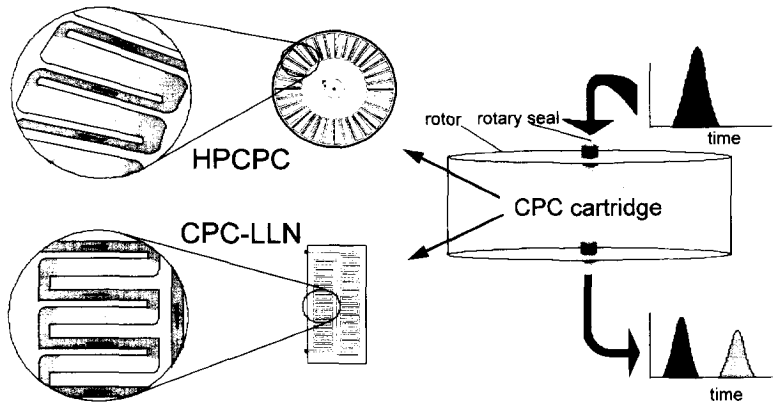

Fig. 1. Schematic drawing of a centrifugal partition chromatograph.

migration velocities and are separated in the column. Some applications for CPC are summarised by Marston and Hostettmann [2].

Margraff [3] mentions the pressure drop as one of the key parameters limiting the scale-up of CPC. The resolution and efficiency of a CPC separation depend on the same variables that determine the pressure drop [4–7]. The direct coupling between the pressure drop and the separation efficiency clearly indicates the need for an accurate model to predict the pressure drop over a CPC column. Berthod and Armstrong [8] have shown experimentally that a considerable pressure drop can arise over the column during CPC separations. According to Berthod and Armstrong the pressure drop is caused by the difference in density between the liquids in the ducts and in the channels and the centrifugal force (hydrostatic contribution), and the friction of the mobile phase with the walls of the channels and ducts (hydrodynamic contribution). The overall pressure drop depends on the flow-rate and rotational frequency (input variables), on the physicochemical properties of the two phases (system variables), on the geometry of the channels and ducts, on the number of channel–duct combinations (apparatus variables) and on the stationary-phase hold-up. The maximum pressure drop is restricted by the rotary seals, which frequently show leakage at prolonged use at high operating pressure (>60 bar). Berthod and Armstrong [8] represented the channels and ducts as a single cylindrical tube with an average diameter. The difference in geometry between a cylindrical tube and the rectangular channels and ducts with different internal diameters was corrected by introducing a geometry parameter. The value of the geometry parameter was determined by comparing the model with 6 experimental pressure drop data points. The geometry parameter showed a spread of 33%. Although, Berthod and Armstrong [8] clearly identify the phenomena that cause the pressure drop over a CPC column, the limited experimental verification (no experimental verification was performed with respect to the influence of the flow-rate, the rotational frequency and the stationary-phase hold-up) makes it difficult to perform an accurate prediction of the pressure drop.

Van Buel et al. [9] presented a model in which the pressure drop is divided into a hydrostatic contribution and a hydrodynamic contribution. The hydrodynamic contribution is further divided into a contribution due to the bends in the channels and ducts and a contribution due to the friction with the walls of the channels and ducts. The model was tested with the heptane–water two-phase system and a single column configuration. The model overestimated the hydrostatic pressure drop, especially at high rotational frequencies. In this work, the model by Van Buel et al. [9] is extended. The extended model is tested for the prediction of the overall pressure drop over two different, laboratory scale CPC columns for a wide range of solvent systems and operating conditions.

2. Model

2.1. Overall pressure drop

The contributions to the hydrodynamic pressure drop are the friction caused by the flow through rectangular channels and ducts ($\Delta P_{friction}$) and the pressure drop due to the bends in the ducts and channels (ΔP_{bend}). The hydrostatic pressure drop (ΔP_{stat}) is due to the density difference between the liquids in the channels and the ducts and the centrifugal acceleration. According to Bernoulli's law the overall pressure drop is equal to the sum of the individual pressure drop contributions. The overall pressure drop ($\Delta P_{overall}$) over the column, consisting of n identical channel–duct combinations, is calculated from:

$$\Delta P_{overall} = n(\Delta P_{stat} + \Delta P_{friction} + \Delta P_{bend}) \quad (1)$$

2.2. Hydrostatic pressure drop

Van Buel et al. [9] showed that the hydrostatic pressure drop is equal to the centrifugal force times the height of the stationary phase in a channel. However, from visual experiments [9] it was concluded that part of the stationary phase is forced into the duct, effectively decreasing the stationary phase height. The total stationary phase height is therefore corrected by introducing a hold-up correction factor, ε_{cor}. The hydrostatic pressure now becomes:

$$\Delta P_{stat} = \Delta\rho\omega^2 R \frac{(\varepsilon_s - \varepsilon_{cor})V}{nA_c} \quad (2)$$

where $\Delta\rho$ is the density difference between the two phases, ω is the rotational frequency, R is the average rotational radius of the cartridge, n is the number of channels–duct combinations, ε_s is the stationary-phase hold-up (the volume of stationary phase divided by the total volume of the column V) and A_c is the cross-sectional area of a channel. Apart from the hold-up correction factor, the hydrostatic pressure drop is now expressed as a function of parameters which can be accessed experimentally. Furthermore, Eq. (2) can be applied for every flow regime. In theory, the hold-up correction factor is a function of the system parameters (e.g. density, viscosity), the input parameters (e.g. flow-rate and rotational frequency) and the apparatus parameters (e.g. channel geometry). The hold-up correction factor for a given two-phase system and a given column can be obtained by fitting experimental pressure drop data obtained under various operating conditions.

The channels of the high-performance CPC (HPCPC) cartridge are tapered (see Fig. 1), which means that the width of the channel changes with the length. In other words, A_c is not constant over the channel. A correction is made by calculating the width of the channel halfway between the position of the interface (between the mobile and the stationary phase) and the top of the channel. This position depends on the stationary-phase hold-up. A_c is calculated from:

$$A_c = d_c\left(w_{entrance} + \frac{\varepsilon_s(w_{exit} - w_{entrance})}{2f_c}\right) \quad (3)$$

in which d_c is the depth of a channel, $w_{entrance}$ and w_{exit} are the width of the entrance and exit of the channel, respectively (depending on ascending or descending mode), and f_c is the fraction of the total column volume that is occupied by the channels.

2.3. Hydrodynamic pressure drop due to friction ($\Delta P_{friction}$)

Following Van Buel et al. [9], the hydrodynamic pressure drop in the rectangular channels and ducts due to the friction with the wall ($\Delta P_{friction}$), is given by:

$$\Delta P_{friction} = \frac{64}{Re}\frac{1}{2}\rho_m v^2 \frac{L}{d_h} 2\zeta \frac{1+\left(\frac{a}{b}\right)^2}{\pi\left(\frac{a}{b}\right)} \quad (4)$$

in which Re is the Reynolds number, ρ_m is the density of the mobile phase, v is the linear velocity of the mobile phase, L is the length of the channel or duct, d_h is the hydraulic internal diameter of the channel or duct, ζ is a correction factor and a and b are the width and the depth of the channel or duct, respectively.

The Reynolds number is given by:

$$Re = \frac{\rho_m v d_h}{\eta_m} \quad (5)$$

in which η_m is the dynamic viscosity of the mobile phase. The hydraulic internal diameter of a rectangular tube is given by:

$$d_h = \frac{2ab}{(a+b)} \tag{6}$$

The linear velocity of the mobile phase is obtained by relating the flow-rate (ϕ_v) to the cross-sectional area of the channel or duct, and correcting for the stationary-phase hold-up:

$$v = \frac{\phi_v}{ab(1-\varepsilon_s)} \tag{7}$$

Cornish [10] gives the following correlation for the correction factor ζ:

$$\zeta = 0.878 + 0.0566\alpha + 0.758\alpha^2 \tag{8}$$

in which α is:

$$\alpha = \frac{1-\frac{b}{a}}{1+\frac{b}{a}} \quad a > b \tag{9}$$

Hydrodynamic pressure drop in rectangular bends (ΔP_{bend})

The pressure drop over a bend is calculated from the following relation [11]:

$$\Delta P_{bend} = K_w \rho_m \frac{v^2}{2} \tag{10}$$

in which K_w is the friction loss factor for the bend. Two types of bends are present in a CPC cartridge: the two bends in the duct with equal inlet and outlet diameters, and the bends in the entrance and exit from the channel to the duct. No correlation seems to exist for K_w, but it is assumed constant for a specific geometry.

3. Materials and methods

The pressure drop experiments were performed with two different types of CPC cartridges.

3.1. CPC–LLN column

A column consisting of two commercially available CPC–LLN 250W cartridges (Sanki Engineering, Japan) was placed in a rotor build by our own workshop. Each cartridge is composed of 4 plates of polychlorotrifluoroethylene (PCTFE). On each side of a plate, 50 channels and ducts in two rows of 25 are engraved. This makes a total of 400 channels and 400 ducts per cartridge, and a total of 800 channels and ducts for a two-cartridge column. Between two plates of PCTFE a sheet of PTFE is placed to seal the cartridge. The geometry and the dimensions of the channels and ducts are shown in Fig. 2. The dimensions were measured with an image analyser after opening the cartridge and filling the channels and duct with a colored solution. The dimensions could be measured with an accuracy of ±0.05 mm. The total length (L) of a duct is 14.59±0.05 mm. The depths of the channels and the ducts were measured with a micrometer. Since PTFE exhibits deformation due to cold flow, part of the PTFE flows into the channels and ducts. Therefore, the depths of the channels and ducts can not be given precisely, but were estimated as 1.15 and 0.95 mm, respectively. The total volume of the two cartridges was determined as 40.4±0.4 ml. The cartridge was placed at two different radii in the rotor (0.21 m and 0.137 m) from the axis to the center of the cartridge, respectively. This was done to check if the radius has an extra effect on the overall pressure drop apart from the effect through the centrifugal acceleration (squared rotational frequency times the radius).

3.2. HPCPC column

A column consisting of a HPCPC 1000 cartridge

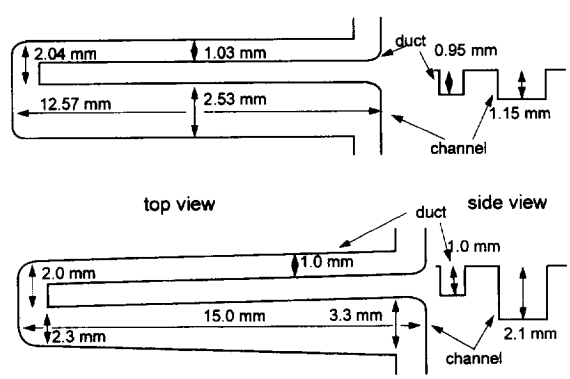

Fig. 2. Construction drawing of the channels and ducts of the CPC–LLN (top) and the HPCPC (bottom) cartridges.

Table 1
Densities and viscosities of the pure liquids used for the single-phase experiments

Liquid	Density (kg/m^3)	Viscosity (mPa s)
Water	998	1.0
n-Heptane	684	0.4
n-Butanol	809	2.8
Tetrachloromethane	1594	0.97

was placed in a rotor obtained from Sanki Engineering. This cartridge consists of two identical parts with 1068 channels and a volume of 103.0±3.0 ml for each part. For the pressure drop experiments, only one part of the cartridge was used (both cartridge parts gave identical results). The geometry and the dimensions are shown in Fig. 2. The dimensions of the channels and ducts were taken from original drawings obtained from Sanki Engineering. The total length (L) of the duct is 17.6±0.05 mm. The distance from the center of the channels to the rotor axis was 0.084±0.001 m.

3.3. Chemicals

Methanol, *n*-butanol, *n*-heptane, ethylacetate and tetrachloromethane were analytical-reagent grade and obtained from J.T. Baker (Deventer, Netherlands). Water was demineralised. The densities and viscosities of the single-phase liquids were taken from Weast [12] and are given in Table 1. The densities of the individual, mutually saturated, phases of the two-phase systems were measured with a Paar DMA 48 density meter. The viscosities of the individual phases of the two-phase systems have been estimated by the method of Teja and Rice [13]. The densities, viscosities and density difference between the phases used in the two-phase experiments are given in Table 2.

3.4. Methods

A schematic drawing of the experimental set-up is given in Fig. 3. To distinguish between the hydrodynamic and the hydrostatic contributions to the overall pressure drop, both single and two-phase experiments were performed. The single-phase experiments were performed by rinsing the column with acetone in the ascending mode at 200 rpm to remove air and traces of earlier phase systems from the column. The column was then filled with the appropriate liquid and, after adjusting the flow-rate to its desired value within the range of 0.5–22.5 ml/min, the pressure drop was measured. The temperature of the column was equilibrated by recycling the liquid through the column at maximum flow-rate until the temperature of the inlet was equal to that of the outlet. All experiments were performed at 25°C. The single-phase experiments were performed in the descending mode at 0 rpm. It was checked however, whether or not the mode and rotational frequency have an influence on the pressure drop for single-

Table 2
Densities, density difference and viscosities for various two-phase systems

Two-phase system (mode)	Density mobile phase (kg/m^3)	Density difference (kg/m^3)	Viscosity mobile phase (mPa s)
Water–*n*-heptane (ascending)	684	314	0.4
Water–*n*-heptane (descending)	998	314	1.0
Water–*n*-butanol (ascending)	848	142	3.5
Water–*n*-butanol (descending)	986	142	1.1
Water–ethyl acetate (ascending)	905	92	0.5
n-Heptane–methanol–water (50:25:25, v/v) (ascending)	926	242	0.4

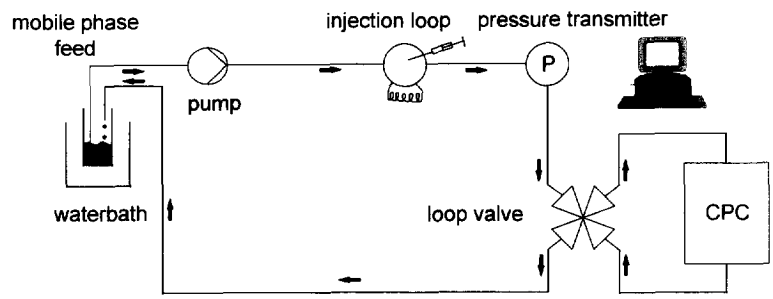

Fig. 3. Schematic drawing of the experimental set-up.

phase experiments. This proved not to be the case. The pressure drop over the appendages apart from the column (tubing, rotary seals) was measured separately and subtracted from the overall pressure drop to obtain the pressure drop over the column.

The pump was a Waters 6000A HPLC pump with extended flow pump heads with a maximum flow of 22.5 ml/min. The pressure transmitters type E 713 were purchased from Bourdon Sedeme. Depending on the maximum pressure reached during an experiment a 6, 10 or 60 bar pressure drop meter was used.

To perform the two-phase experiments, the column was first rinsed with acetone in the ascending mode at 200 rpm to remove air and traces of previous phase systems from the column. Then the column was filled with the stationary phase. Subsequently, the loop valve was closed and the volume outside the loop was rinsed with acetone and filled with the mobile phase. Since the volume of the column and the volume of the connecting tubes and other appendages (rotary seals) before and after the loop valve were also measured, it is possible to calculate the stationary-phase hold-up. After setting the correct mode (ascending or descending) and the required rotational frequency and flow-rate, the loop valve was opened. The volume of stationary phase pushed out of the column was measured with a burette. The temperature of the column was equilibrated by putting the mobile phase flask in a temperature bath and recycling the mobile phase. All experiments were performed at 25°C. The pressure drop was measured as a function of either the rotational frequency or the flow-rate, while keeping the other constant. The rotational frequency was varied between 200–1600 rpm, constrained by flooding of the column at low rotational frequencies, and leakage of the rotary seals at high rotational frequencies. The flow-rate was varied between 0.5–10 ml/min. The flow-rates and rotational frequencies used during the experiments were lower and higher, respectively, than those used during the filling of the column with the mobile phase. This was done to prevent bleeding of stationary phase from the column, during the experiments. The mobile and stationary phases were prepared by mixing the liquids thoroughly and allowing the two phases to saturate and settle overnight. The pressure drop over the appendages apart from the column (tubing, rotary seals) was measured separately and subtracted from the overall pressure drop to obtain the pressure drop over the column. A list of the experiments that were performed is given in Table 3.

4. Results and discussion

4.1. Single-phase pressure drop

For the single-phase pressure drop experiments, only the hydrodynamic contributions are considered. In that case the single unknown parameter in Eq. (1) is the friction loss factor for the bends (K_w, see Eq. (10)). Assuming that K_w is not a function of Reynolds, it was estimated by fitting Eq. (1) to the single-phase experimental pressure drop data of a large set of liquids with different viscosities and densities. K_w is a parameter in which all contributions of the bends of a channel-duct combination are lumped, making K_w specific for channels and ducts with a given geometry. The result of fitting the

Table 3
Summary of pressure drop experiments with experimental conditions (a = ascending, d = descending)

	Column type	Liquids	Mode	Conditions ϕ_v (ml/min), ω^2R (rad^{2}m/s^2), ε_s
Single phase	CPC–LLN	water, ethanol, tetra *n*-heptane, ether, *n*-butanol	–	$1<\phi_v<22.5$ except for *n*-butanol $1<\phi_v<17.5$ due to pressure drop limitation
Two phase	CPC–LLN	water–*n*-heptane	a/d	$5<\phi_v<19$, $500<\omega^2R<3000$, $0.35<\varepsilon_s<0.53$
		water–ethyl acetate	a	$5<\phi_v<15$, $3000<\omega^2R<5400$, $0.19<\varepsilon_s<0.54$
		water–*n*-butanol	d	$5<\phi_v<10$, $1000<\omega^2R<5400$, $0.10<\varepsilon_s<0.60$
		water–methanol–*n*-heptane (25:25:50)	d	$\phi_v=5$, $500<\omega^2R<3900$, $0.40<\varepsilon_s<0.61$
Single phase	HPCPC	water, ethanol, acetone, 2-propanol, *n*-butanol, *n*-heptane, ether, ether	–	$1<\phi_v<20$
Two phase	HPCPC	water–*n*-heptane	a/d	$2<\phi_v<8$, $200<\omega^2R<1200$, $0.71<\varepsilon_s<0.75$
		water–*n*-butanol	a/d	$\phi_v=1$, $300<\omega^2R<2500$, $0.54<\varepsilon_s<0.76$
		methanol–*n*-heptane	d	$\phi_v=1$, $150<\omega^2R<2500$, $0.23<\varepsilon_s<0.74$

single-phase experimental pressure drop data (per channel–duct combination) for the CPC–LLN cartridge for water, *n*-heptane, tetrachloromethane and *n*-butanol is shown in Fig. 4. The model gives an adequate prediction of the pressure drop as a function of the flow-rate for four different liquids with a constant value for K_w of 5.2.

Since the geometry and the dimensions of the channels and duct in the HPCPC cartridge are different from the CPC–LLN cartridge the K_w is expected to be different. Fig. 5 shows single-phase experimental pressure drop data (per channel-duct combination) for the HPCPC cartridge for water, *n*-heptane, tetrachloromethane and *n*-butanol. By fitting the experimental data with the model, a K_w of 6.0 was obtained. The slightly higher K_w for the HPCPC cartridge can be explained by the difference in the geometry at the in- and outlet of the channel. In case of the HPCPC cartridge, the depth of the duct is only 50% of the depth of the channel, while for the CPC–LLN cartridge this is roughly 90%. Nevertheless, the influence of the geometry on K_w is small.

Comparing Fig. 4 with Fig. 5 shows that the hydrodynamic pressure drop per channel–duct

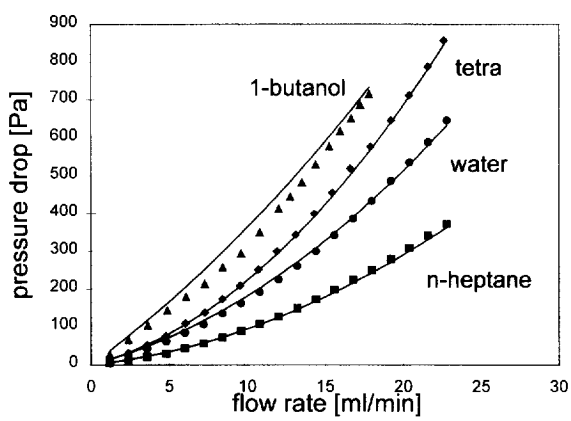

Fig. 4. Hydrodynamic pressure drop (per channel–duct combination) as a function of the flow-rate for various liquids for the CPC–LLN cartridge. Markers are experimental data, lines are model predictions.

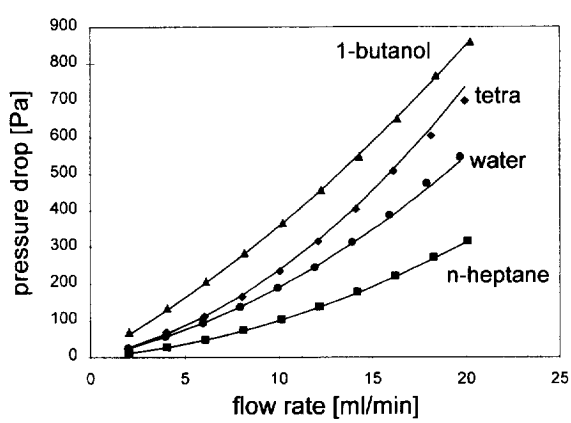

Fig. 5. Hydrodynamic pressure drop (per channel–duct combination) as a function of the flow-rate for various liquids for the HPCPC cartridge. Markers are experimental data, lines are model calculations.

combination for the HPCPC cartridge is almost equal to that of the CPC–LLN cartridge (±0–10%, depending on the flow-rate and the liquid that is used). The higher K_w for the HPCPC cartridge is compensated by the slightly larger ducts height and width.

From the system parameters, the viscosity has the largest influence on the hydrodynamic pressure drop. A change of 5% in viscosity changes the hydrodynamic pressure drop with 4.5%. The density has a smaller effect on the hydrodynamic pressure drop, however, for liquids with a high density like tetrachloromethane it becomes important. Since tetrachloromethane and water have almost the same viscosity, the higher pressure drop at higher flow-rates for tetrachloromethane is caused by its higher density. The dimensions of the ducts have the largest influence on the hydrodynamic pressure drop. A variation of 25% in duct height or width, equal to the accuracy of the dimensions, changes the hydrodynamic pressure drop with 15%.

The various contributions of the channels and ducts to the hydrodynamic pressure drop are not equal. Fig. 6 shows the three contribution to the total hydrodynamic pressure drop as a function of the flow-rate for water. With the liquids commonly used in CPC separations, such as water, hydrocarbons and lower alcohols [14], the bends and the ducts contribute for at least 90–95% to the total hydrodynamic pressure drop. The pressure drop over the channels is almost negligible. The exact percentage to which the three terms contribute to the total hydrodynamic pressure drop depends on the flow-rate, the viscosity and the density. The pressure drop over the bends is more important at lower viscosities and higher flow-rates. The average deviations between the experimental data points and the model predictions for the single-phase experiments are 6.5% and 4.2% for the CPC–LLN and the HPCPC cartridges, respectively.

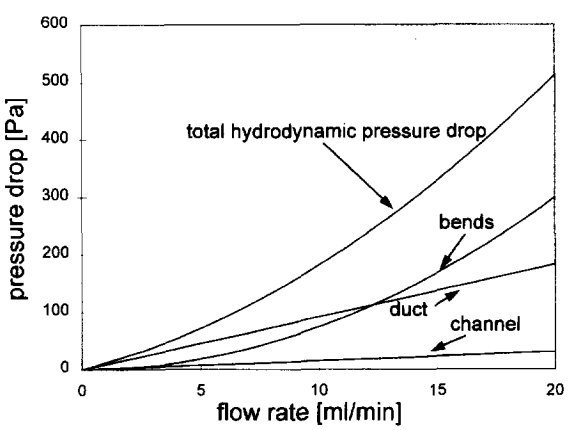

Fig. 6. Simulated pressure drop contributions to the total hydrodynamic pressure drop (per channel–duct combination) as a function of the flow-rate for water for the CPC–LLN cartridge.

4.2. Two-phase pressure drop

To validate the pressure drop model for two-phase systems, experiments with several two-phase systems with different physicochemical properties (densities, viscosities and interfacial tensions) were performed in the ascending and the descending mode. For the two-phase pressure drop both the hydrodynamic and the hydrostatic pressure drop are taken into account.

Experiments with the CPC–LLN cartridge at two different radii in the rotor show that the pressure drop as a function of the centrifugal acceleration is equal for the two radii. Therefore, the centrifugal acceleration ($\omega^2 R$) is used as the parameter that determines the hydrodynamic pressure drop rather than the rotational frequency and the radius separately.

To determine the influence of the different parameters on the hold-up correction factor, experiments with the CPC–LLN cartridge for four different two-phase systems in the ascending and the descending mode, for various flow-rates and rotational frequencies were performed. For each two-phase system, a hold-up correction factor was fitted. Fig. 7 shows model predictions of the overall pressure drop (per channel-duct combination) with and without the hold-up correction factor as a function of the centrifugal acceleration ($\omega^2 R$) for 2 two-phase systems for the same flow-rate and stationary-phase hold-up. Fig. 7 shows that the model gives a good representation of the experimental data points for the CPC–LLN cartridge, if the hold-up correction factor is applied. The hold-up correction factor is only a small correction to the overall pressure drop, between 4% (for the ethylacetate–water system) and maximum 10% (for the heptane–water system), depending on the stationary-phase hold-up, while the average deviation between the experimental data points and

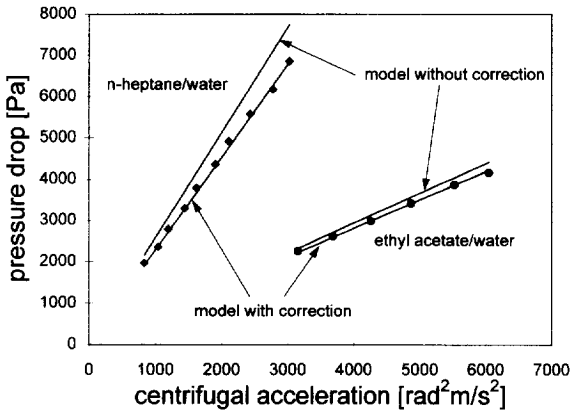

Fig. 7. Overall pressure drop (per channel–duct combination) as a function of the centrifugal acceleration for the CPC–LLN cartridge in the ascending mode. Markers are experimental points, lines are model predictions.

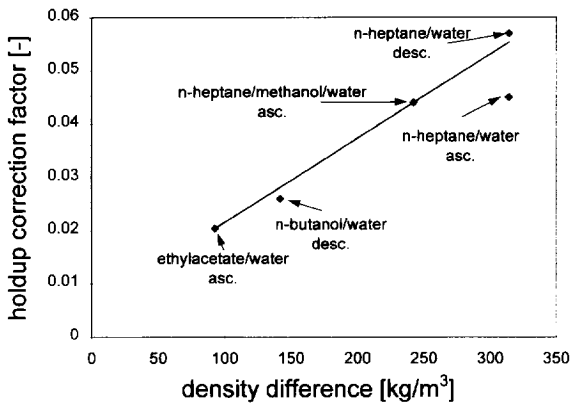

Fig. 8. Fitted hold-up correction factor as a function of the density difference for various two-phase systems for the CPC–LLN cartridge. The line is calculated from Eq. (11).

the model prediction (with the hold-up correction factor) for the two-phase experiments is 4.5%. However, we still believe that the hold-up correction factor is the best way for correcting the consistent positive deviation for the CPC–LLN cartridge, given the clear visual verification that part of the stationary phase is present in the duct. The fact that the influence of the hold-up correction factor is of the same order as the difference between the model predictions and the experimental data makes it very difficult to determine the influence of the various system and input variables on the hold-up correction factor. However, we found that the hold-up correction factor did hardly vary with flow-rate or centrifugal acceleration. Furthermore, it was possible to obtain a satisfactory result by correlating the hold-up correction factor with the density difference of the phases. Fig. 8 shows the fitted hold-up correction factor as a function of the density difference between the phases. The linear relation between the fitted hold-up correction factors and the density difference between the two phases can be described by:

$$\varepsilon_{cor} = 0.00587 + 0.000157\Delta\rho \qquad (11)$$

The difference in hold-up correction factor between the water–*n*-heptane system in the ascending and the descending mode might be explained by the fact that the difference is smaller than the average difference between the model predictions and the experimental data points. For all subsequent model predictions for the CPC–LLN cartridge, the fitted hold-up correction factor calculated by Eq. (11) was applied.

The maximum amount of stationary phase that can flow into the ducts for the HPCPC cartridge is maximum 4% of the total channel volume. Visually, it was observed that again only half of the duct, maximum, is filled with the stationary phase. This means that the maximum hold-up correction will only be 2%. This is within the error of the determination of the hold-up and the volume of the column. It was therefore decided not to use the hold-up correction factor for the HPCPC cartridge.

Fig. 9 shows the experimental and the predicted pressure drop for the HPCPC cartridge for the *n*-heptane–water and the *n*-butanol–water two phase system in the ascending and the descending mode at 2 ml/min as a function of the centrifugal frequency. It shows that the model (without the hold-up correction factor) gives a fair prediction of the pressure drop. This means that it is indeed not necessary to use the hold-up correction factor for the HPCPC cartridge.

Figs. 7 and 9 show that the overall pressure drop (per channel–duct combination) is a strong function of the centrifugal acceleration. The overall pressure drop (per channel–duct combination) is maximum for systems with a high difference in density between the phases. By comparing the maximum single-phase pressure drop (Figs. 4 and 5) to the maximum two-phase pressure drop (Figs. 7 and 9) it can be

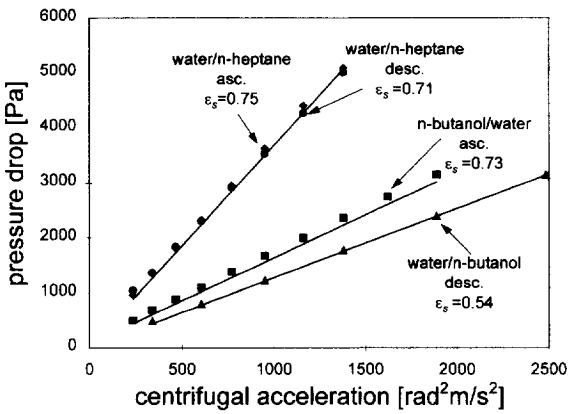

Fig. 9. Pressure drop (per channel–duct combination) as a function of the centrifugal acceleration for the HPCPC cartridge. Markers are experimental date, lines are model predictions ($\phi_v = 2$ ml/min).

seen that the hydrodynamic pressure drop is small compared to the overall pressure drop, especially for low flow-rates and high centrifugal accelerations.

Eq. (4)– Eq. (10) for the hydrodynamic contributions are based on the assumption of single-phase flow. The two-phase system in the channels, however, might influence the single-phase hydrodynamic pressure drop. To find out whether this is true, single-phase pressure drop data were compared to the two-phase pressure drop data. This is shown in Fig. 10 where the overall pressure drop (per channel–duct combination) as a function of the flow-rate is given for a single-phase pressure drop experiment with the mobile phase of the water–*n*-heptane system and for a two-phase pressure drop experiments (descending mode) with the same system at 3 different rotational frequencies. The error bars indicate the average deviation of 6.5% between the single flow experiments and the model predictions. Fig. 10 shows that the model predictions are within the indicated error bars. This indicates that the single-phase hydrodynamic pressure drop model is also valid for predictions of the overall pressure drop when a second phase is present in the channels. This can be explained by the fact that the stationary phase is mainly present in the channels. It has already been shown that the contributions due to the ducts and the bends are the main contributions to the hydrodynamic pressure drop. This means that even if there is an influence of the stationary phase on the hydrodynamic pressure drop of the mobile phase in the channel the influence on the overall pressure drop will be small.

Fig. 11 shows the overall pressure drop as a function of the centrifugal acceleration for the CPC–LLN cartridge for various stationary-phase hold-ups for the water–*n*-butanol system (descending mode). Again the model gives a good prediction of the overall pressure drop. Fig. 11 shows that the overall

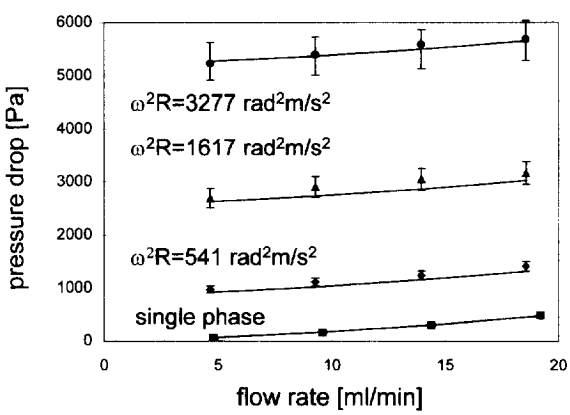

Fig. 10. Overall pressure drop (per channel–duct combination) as a function of the flow-rate for the *n*-heptane–water two-phase system in the descending mode for the CPC–LLN cartridge. Markers are experimental data, lines are model predictions ($\varepsilon_s = 0.27$).

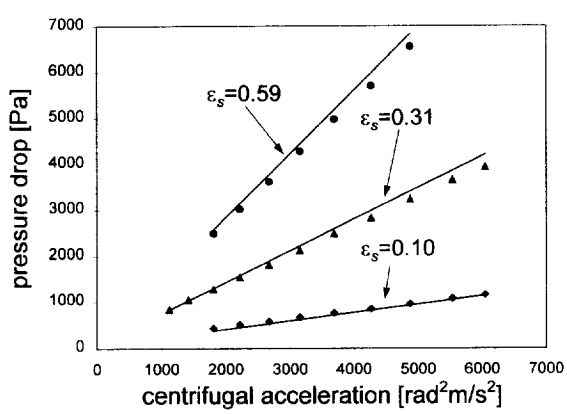

Fig. 11. Overall pressure drop (per channel–duct combination) as a function of the centrifugal acceleration for *n*-butanol–water in the descending mode for three stationary phase hold-ups for the CPC–LLN cartridge. Markers are experimental data, lines are model predictions ($\phi_v = 4.7$ ml/min).

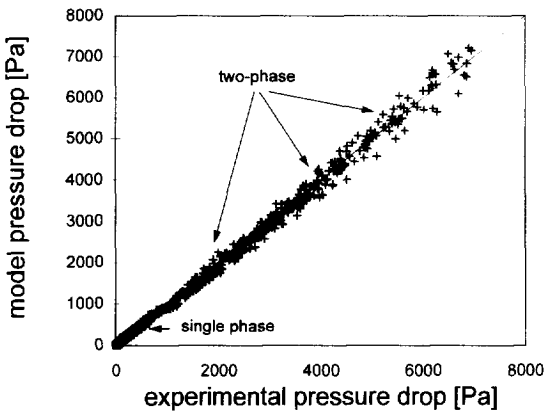

Fig. 12. Parity plot for single-phase and two-phase experiments (pressure drop per channel–duct combination) for the CPC–LLN and HPCPC column.

pressure drop increases with the stationary-phase hold-up.

Fig. 12 shows a parity plot for 372 two-phase experimental pressure drop data points for five different two-phase systems for various flow-rates and rotational frequencies and 193 single-phase experimental data points for six different single-phase systems. Fig. 12 shows that the pressure drop model gives a good prediction of the overall pressure drop.

The average deviation between the experimental points and the model prediction for the HPCPC cartridge for the two-phase experiments was 6.4%. It should be kept in mind that the model only predicts the pressure drop over the cartridges. Any additional pressure drop due to the tubing and appendages should be measured separately.

5. Conclusions

A predictive model for the pressure drop over a CPC column is presented. The model contains two pressure drop contributions; a hydrostatic and a hydrodynamic. The model can be used to predict the overall pressure drop as a function of the flow-rate of the mobile phase, the centrifugal acceleration, the stationary-phase hold-up and the physicochemical properties of the phases. The model was validated for two column geometries. The model contains two parameter (K_w, ε_{cor}) and predicts the single-phase hydrodynamic pressure drop with an average deviation of 6.5% and 4.2% for the CPC–LLN and the HPCPC cartridge respectively. The model predicts the overall pressure drop with an average deviation of 4.5% and 6.4% for the CPC–LLN and the HPCPC cartridge respectively.

The hydrodynamic pressure drop is mainly due to the viscous flow through the ducts and the bends in the ducts. The two important parameters which influence the hydrodynamic pressure drop as a function of the flow-rate are the dimensions of the ducts and the viscosity of the liquid phases. The model for the hydrodynamic pressure drop, which is based on the assumption of single-phase flow also applies for two-phase flow. The hydrodynamic pressure drop is independent of the centrifugal acceleration, as is predicted by the model. The overall pressure drop is mainly caused by the hydrostatic pressure drop (>80%), specially for two-phase systems with a low mobile phase viscosity and a high density difference.

6. Notation

a	width of a channel or duct (m)
A_c	cross-sectional area (m^2)
b	depth of a channel or duct ($a>b$) (m)
d_h	hydraulic diameter according to Eq. (6) (m)
d_c	depth of a channel (m)
f_c	fraction of column volume taken by channels
K_w	friction loss factor
L	length of the channel or duct (m)
n	overall number of channel-duct combinations
R	average rotation radius of the cartridge (m)
Re	Reynolds number
ΔP	pressure drop (Pa)
v	linear velocity of the mobile phase according to Eq. (7) (m/s)
V	total volume of the column (m^3)
w	width of channel (m)
Greek	
ρ_m	density of the mobile phase (kg/m^3)
$\Delta\rho$	density difference between the phases (kg/m^3)

ε_s	stationary-phase hold-up (m^3/m^3)
ε_{cor}	hold-up correction factor
ζ	correction factor depending on a and b
η_m	dynamic viscosity of the mobile phase (Pas)
ϕ_v	flow-rate (m^3/s)
ω	rotational frequency (rad/s)

Acknowledgments

The Center of Bio-Pharmaceutical Sciences, Division of Pharmacognosy, of the Leiden University is gratefully acknowledged for providing the CPC–LLN cartridges. The technicians of the workshop and electronics department of the Kluyver Laboratory for Biotechnology are thanked for constructing the CPC equipment.

References

[1] A.P. Foucault, CPC Instrumentation, in A.P. Foucault (Editor), Centrifugal Partition Chromatography, Wiley, New York, 1995, pp. 355–362.
[2] A. Marston, K. Hostettmann, J. Chromatogr. 658 (1994) 315–341.
[3] R. Margraff, in A.P. Foucault (Editor), Centrifugal Partition Chromatography, Wiley, New York, 1995, pp. 331-353.
[4] W. Murayama, T. Kobayashi, Y. Kosuge, H. Yano, Y. Nunogaki, K. Nunogaki, J. Chromatogr. 239 (1982) 643–649.
[5] D.W. Armstrong, G.L. Bertrand, A. Berthod, Anal. Chem. 60 (1988) 2513–2519.
[6] A.P. Foucault, O. Bousquet, F. Le Goffic, J. Liq. Chromatogr. 15 (1992) 2691–2706.
[7] M.C. Rolet, D. Thiebaut, R. Rosset, Analusis 20 (1992) 1–11.
[8] A. Berthod, D.W. Armstrong, J. Liq. Chromatogr. 11 (1988) 546–583.
[9] M.J. van Buel, L.A.M. van der Wielen and K.Ch.A.M. Luyben, in A.P. Foucault (Editor), Centrifugal Partition Chromatography, Wiley, New York, 1995, pp. 51–69.
[10] R.J. Cornish, Proc. Roy. Soc. London (A) 120 (1928) 691–700.
[11] H. Brauer, Grundlagen der Einphasen- und Mehrphasenströmungen, Sauerländer, Aarau/Frankfurt am Main, 1972.
[12] R.C. Weast (Editor), CRC Handbook of Chemistry and Physics, CRC Press, Boca Raton, FL, 1980.
[13] A.S. Teja, P. Rice, Ind. Eng. Chem. Fundam. 20 (1981) 77–81.
[14] A.P. Foucault, Anal. Chem. 64 (1991) 569A–579A.